LeiCNS-PK3.2: a physiologically based pharmacokinetic model framework for predicting intracellular concentrations of acyclovir and ganciclovir active metabolites

Sun, M.; Manson, M.L.; Guo, T.; Lange, E.C.M. de

European Journal of Pharmaceutical Sciences 221 (2026) 107496

Contents lists available at ScienceDirect

European Journal of Pharmaceutical Sciences

journal homepage: www.elsevier.com/locate/ejps

LeiCNS-PK3.2: A physiologically based pharmacokinetic model framework for predicting intracellular concentrations of acyclovir and ganciclovir active metabolites

Ming Sun, Martijn L. Manson, Tingjie Guo, Elizabeth C.M. de Lange *

Systems Pharmacology and Pharmacy, Leiden Academic Centre for Drug Research (LACDR), Leiden University, Leiden, Netherlands

ARTICLE INFO

Keywords:
Acyclovir
Ganciclovir
Nucleoside analogues
Intracellular pharmacokinetics
CNS infection
Central nervous system (CNS) pharmacokinetics
Physiologically-based pharmacokinetic (PBPK) modeling

ABSTRACT

Background: Effective treatment of viral infections in the central nervous system (CNS) requires adequate nucleoside analogs exposure and conversion into phosphorylated metabolites (TP) in brain cells.
Aim: To develop a CNS PBPK model (LeiCNS-PK3.2) that incorporates active brain cell membrane transport and brain intracellular fluid (brainICF) metabolism to predict and understand target site pharmacokinetics (PK), brainICF active triphosphate (TP) metabolites, and effects of antiviral drugs.
Method: LeiCNS-PK3.0 was extended with a brain cell membrane asymmetry factor (AF) using rat-derived $K_{p,uu,cell}$ values. Intracellular conversion of acyclovir and ganciclovir into TPs was modelled using *in vitro* kinetic parameters. LeiCNS-PK3.2 was validated on published rat and human plasma, brain extracellular fluid (brainECF), and cerebrospinal fluid (CSF) data. Simulated PK profiles for parent drug standard dosing regimens (acyclovir 10 mg/kg t.i.d.; ganciclovir 5 mg/kg b.i.d.) were compared to parent-drug profiles in brainECF, and TP metabolite in brainICF. Sensitivity analyses were performed on CNS physiological parameters and $K_{p,uu,cell}$ values.
Results: LeiCNS-PK3.2 accurately recaptured the observed data (<2-fold error range). Simulated brainECF parent drug concentrations often remained below reported IC_{50} values, whereas brainICF TPs had smaller AUCs and longer time to equilibrium compared to acyclovir/ganciclovir in brainECF. Simulated pathological variations during CNS infection showed minimal impact on brainICF TP exposure, with proportional shifts in brainICF TP concentrations when varying $K_{p,uu,cell}$.
Conclusions: LeiCNS-PK3.2 can predict CNS target-site exposure of TPs and demonstrates that brainECF acyclovir/ganciclovir concentrations are distinct from brainICF TP levels. It may support intracellular PK/PD target determination to optimize dosing strategies for CNS viral infections.

1. Introduction

Nucleoside analogs are a wildly used class of antivirals for treating various viral infections. Depending on the primary site of infection, viral infections can be classified as general infection affecting systemic circulation or local infections where specific organs or tissues are involved (CJ et al., Virology, 2017). Among these, viral infections of the central nervous system (CNS) are rare but life-threatening disease, characterized by viruses invading brain parenchymal cells and trigger inflammatory reactions within the CNS (Sun, et al., CNS Drugs, 2024). Compared to systemic infections, CNS infection poses unique challenges for antiviral therapy. One major obstacle is the presence of CNS barriers including the blood-brain barrier (BBB) and the blood-cerebrospinal fluid barrier (BCSFB), both of which hinder drug penetration and limit pharmacologically effective concentrations in the CNS (de Lange, et al., Clinical Pharmacology and Therapeutics, 2022). In case drugs cross these CNS barriers, the complex CNS architecture further affects the drug distribution and exposure in the target region, intracellular space of brain cells where viral replication occurs (de Lange, Fluids Barriers CNS, 2013).

Pharmacokinetic (PK) studies are essential for investigating drug distribution and exposure levels at the CNS site of action to optimize antiviral dosing. However, most PK studies of antivirals focus on plasma drug concentrations, providing limited insight into CNS-specific PK.

* Corresponding author.
E-mail address: ecmdelange@lacdr.leidenuniv.nl (E.C.M. de Lange).

https://doi.org/10.1016/j.ejps.2026.107496
Received 16 December 2025; Received in revised form 2 March 2026; Accepted 3 March 2026
Available online 6 March 2026

When CNS exposure is assessed, it is often inferred from cerebrospinal fluid (CSF) measurements, yet CSF levels may not accurately represent drug concentrations in brain extracellular fluid (brainECF), and more critically, in brain intracellular fluid (brainICF). Our recent work demonstrated significant PK disparities among plasma, CSF, and brainECF (Sun, et al., Clinical Pharmacokinetics, 2025). Although the brainECF concentrations are considered physiologically closer to brainICF than plasma or CSF, it still cannot simply be assumed that drug distribution between brain ICF and ECF is uniform and homogeneous. Antivirals must cross the brain cell membrane, where the lipid bilayer may retain drugs through nonspecific binding based on drug's lipophilicity (Vendel, et al., Fluids and Barriers of the CNS, 2019). Additionally, active transporters expressed on brain cell membranes might regulate drug influx and efflux (Lee, et al., Pharmacological Reviews, 2001). Finally, antiviral nucleoside must undergo intracellular phosphorylation to form their active triphosphate (TP) metabolites to exert antiviral effects (Sun, et al., CNS Drugs, 2024). Given these mechanisms involved, the PK of an antiviral nucleoside within brain cells may differ markedly from that in other compartments, so arbitrarily extrapolating from non-target measurements is not scientifically based.

Nevertheless, direct measurement of these metabolites in human brain cells remains technically challenging. Although microdialysis is the gold-standard technique for obtaining the unbound CNS drug concentrations, it is invasive and ethically prohibitive for use in healthy volunteers or most patients without a neurosurgical indication (Yamamoto, et al., The AAPS Journal..2017). Although imaging techniques such as positron emission tomography (PET) can offer some insight by measuring the total drug concentration in the brain, it cannot distinguish between parent drugs and active metabolites (Zhang, et al., Drug MeTable Dispos, 2019). *In vitro* cell models are commonly used to reveal PKs of active triphosphate metabolites in virus-infected cells, however, these systems lack the physiological and structural complexity of the CNS compared to *in vivo* systems and hence would benefit from integration with mathematical modeling approaches for comprehensive PK analysis (Pertinez, et al., J Antimicrob Chemother, 2021; Zhang, et al., European Journal of Pharmaceutical Sciences: Official Journal of the European Federation For Pharmaceutical Sciences, 2024).

Physiologically based pharmacokinetic (PBPK) modeling offers a powerful method to predict drug distribution across various organs and tissues, including intricate CNS compartments. Our previous model, LeiCNS-PK3.0, well captured the distribution of drugs within multiple CNS regions (Saleh, et al., J Pharmacokinet Pharmacodyn, 2021a). However, it only accounted for passive diffusion across brain parenchymal cell membranes. For nucleoside analogs specifically, it is crucial to incorporate intracellular conversion processes into the model, as only their phosphorylated active metabolites exert antiviral activity, not the parent drugs. Furthermore, because direct measurement of drug and metabolite concentrations within human brain tissues to observe their dynamic changes over time is ethically infeasible, predictive CNS PBPK models serve as an essential tool to bridge this gap. By integrating *in vitro* data on active metabolites and considering active transport mechanisms at the brain cell membrane, our model would hence provide more comprehensive understanding on target site PK.

In this study, we aimed to develop LeiCNS-PK3.2, an extension of LeiCNS-PK3.0 model, that incorporates active transport mechanisms on brain cell membranes as well as intracellular conversion of acyclovir and ganciclovir into active metabolites. By integrating data from diverse sources, we predicted the intracellular active metabolite concentrations of our model drugs, acyclovir and ganciclovir and analyzed the potential PK discrepancies between the target site (brainICF) and non-target site (brainECF).

2. Methods

The present model represents one of several parallel extensions derived from the original LeiCNS-PK3.0 framework. Within our group, multiple expansions and adaptations have been developed to address different research objectives, and these have not all been published sequentially. The name LeiCNS-PK3.2 was adopted to distinguish the implementation for current CNS infection within this evolving framework.

2.1. Incorporation of active transport across brain cell membranes

In LeiCNS-PK3.0, physiological processes such as active transport across the BBB and BCSFB are incorporated into the model using the so-called asymmetry factors (AF_{in} and AF_{out}). The AF terms, including AF_{ECF} (representing the brainECF), AF_{LV} (representing the lateral ventricle), and AF_{TFV} (representing the third and fourth ventricle), are calculated based on the LeiCNS PK3.0 equations (Saleh, et al., J Pharmacokinet Pharmacodyn, 2021a) together with $K_{p,uu,BBB}$ or $K_{p,uu,BCSFB}$, which describe the steady state ratio of unbound drug concentration in specific CNS compartments (brainECF, lateral ventricle, and third and fourth ventricles) relative to plasma (Hammarlund-Udenaes, et al., Pharm Res, 2008). To further extend drug active transport across brain cell membrane, in LeiCNS-PK3.2 we introduced a new AF_{BCM} based on $K_{p,uu,cell}$, defined as the unbound concentration ratio at steady state between brainECF and brainICF. The impact of the net effect of active transporters on drug exchange at the BBB, BCSFB, and the brain cell membrane was incorporated using $AF_{in,ECF/LV/TFV/BCM}$ and $AF_{out,ECF/LV/TFV/BCM}$. These factors were derived from $K_{p,uu,BBB/BCSFB/Cell}$ values such that they produced the same $K_{p,uu,BBB/BCSFB/Cell}$ values within the PBPK model at steady-state. Thus, the $AF_{ECF/LV/TFV/BCM}$ is dependent on both the $K_{p,uu,BBB/BCSFB/Cell}$ values and the specific structure and parameters of the PBPK model. The derivation of $AF_{ECF/LV/TFV/BCM}$ depends on the direction of net transport: for net active influx ($K_{p,uu,BBB/BCSFB/Cell} > 1$), $AF_{in,ECF/LV/TFV/BCM}$ is derived from $K_{p,uu,BBB/BCSFB/Cell}$ while $AF_{out,ECF/LV/TFV/BCM}$ is fixed at 1; for net active efflux ($K_{p,uu,BBB/BCSFB/Cell} < 1$), $AF_{out,ECF/LV/TFV/BCM}$ is derived from $K_{p,uu,BBB/BCSFB/Cell}$, while $AF_{in,ECF/LV/TFV/BCM}$ is fixed at 1. In our analysis, $K_{p,uu,BBB/BCSFB/Cell}$ values for the BBB and BCSFB were obtained from existing *in vivo* data using either unbound AUC ratios or concentration ratios from brainECF or CSF to plasma.

To obtain the values of $K_{p,uu,cell}$ for each drug, we used the following equations to calculate (Eq. 1&2) (Loryan, et al., Fluids and Barriers of the CNS, 2013).

$$K_{p,uu,cell} = V_{u,brain} * f_{u,brain} = \frac{A_{tot,brain} - V_{blood} * C_{blood}}{C_{u,brainECF}} * f_{u,brain} \quad (1)$$

$$V_{u,brain} = \frac{K_{p,brain}}{K_{p,uu,brain,ECF} * f_{u,plasma}} \quad (2)$$

Here, $V_{u,brain}$ denotes the unbound volume of distribution in brain (mL per g brain), and $f_{u,brain}$ represents the unbound fraction in brain tissue. Brain density was assumed to be 1 g per mL so that $K_{p,uu,cell}$ could be obtained from $V_{u,brain}$ by accounting for tissue binding while maintaining a unitless definition (Bällgren, et al., Fluids Barriers CNS, 2025). For ganciclovir, $V_{u,brain}$ was calculated using published data (Liu, et al., Drug MeTable Dispos, 2009) based on Eq. (1), where $V_{u,brain}$ can be calculated using the total drug amount in the brain $A_{tot,brain}$(nanomoles per g brain), corrected for the contribution of blood (V_{blood}·C_{blood}), normalized to the unbound steady-state concentration in the brainECF ($C_{u,brainECF}$, nanomoles per mL) (Wang, et al., Pharmaceutical Research, 1996). V_{blood} is the physiological volume (mL) of blood in brain per g brain weight (3 % or less) (Khor, et al., Drug MeTable Dispos, 1991). The relevant $f_{u,brain}$ value was reported in the same publication (Liu, et al., Drug MeTable Dispos, 2009) which utilized brain homogenate dialysis. However, no directed information on $V_{u,brain}$ and $f_{u,brain}$ were available regarding acyclovir. Therefore, its relevant parameters were predicted via the online platform DruMAP (version 1.5, https://drumap.nibiohn.go.jp), which uses drug physicochemical properties (pKa, pKb, logP,

and molecular structure) as input. In DruMAP, $f_{u,brain}$ is directly predicted, whereas $V_{u,brain}$ is further calculated using the predicted parameters including the ratio of the brain-to-plasma partition coefficient ($K_{p,brain}$), the unbound brain-to-plasma drug partition coefficient ($K_{p,uu,brainECF}$), and the unbound fraction in plasma ($f_{u,plasma}$) (Eq. (2)) (Loryan, et al., Pharm Res, 2022). The steady-state differential equations were solved using the Maxima Computer Algebra System (http://maxima.sourceforge.net) to obtain algebraic solutions for the AFs, the details of which are provided in Supplementary File. These AFs were then applied to the passive transcellular diffusion parameters at the BBB, BCSFB, and brain cell membrane ($Q_{t,BBB}$, $Q_{t,BCSFB}$, $Q_{t,BCM}$) within the model to incorporate active transport mechanism.

Importantly, the data that we collected to calculate the $K_{p,uu,cell}$ were all from rat. Since there are no available data to indicate the human corresponding values, we assumed equal values for human and rat and used the rat values for the human model development.

2.2. Incorporation of intracellular active conversion of acyclovir and ganciclovir

For both acyclovir and ganciclovir, the intracellular PK of their TPs were modeled under the assumption of instantaneous conversion from the parent drug to its triphosphate form, consistent with *in vitro* observations showing low or undetectable mono- and di-phosphate intermediates (Gentry, et al., Antimicrob Agents Chemother, 2014; Sauer, et al., Antiviral Res, 2020). The Intracellular conversion process was represented with a one-compartment model with first-order kinetics (Eq. (3)).

$$\frac{dC_{TP}}{dt} = k_{form}C_{parent} - k_{elim}C_{TP} \quad (3)$$

where the elimination rate constant k_{elim} was fixed based on literature-reported half-life values of 27 h for acyclovir-TP and 37 h for ganciclovir-TP, respectively (Gentry, et al., Antimicrob Agents Chemother, 2014; Sauer, et al., Antiviral Res, 2020). The TP formation rate constant k_{form} was calculated using Eq. (4) under steady state condition:

$$k_{form} = \frac{C_{TP,ss}}{C_{parent,ss}} * k_{elim} \quad (4)$$

where $C_{TP,ss}$ and $C_{parent,ss}$ refer to the observed concentrations for the TP and parent drug at the steady state, respectively. The steady state concentrations of parent drugs and TPs were extracted from the final measurement time point of the incubation period. Reported TP concentrations (pmol per million cells) were converted to μM using cell-specific volumes: 6.4 μL for 1 million Vero cells (da Silva, et al., Cell Prolif, 2010) and 4 μL for 1 million human foreskin fibroblasts (HFFs) (Angello, et al., Journal of Cellular Physiology, 1987). We assumed acyclovir/ganciclovir enter cells predominantly via passive diffusion across the tested cell lines (*e.g.*, Vero cell and HFFs), since no transporters specific to these drugs have been identified in these cell lines Therefore, the unbound intracellular parent drug concentration at steady state was approximated by the unbound medium concentration. At the end, the formation and elimination rate constants obtained from *in vitro* intracellular data were incorporated into LeiCNS-PK3.2 model.

2.3. LeiCNS-PK3.2 model building

Based on the LeiCNS-PK3.0 modeling framework, we constructed our model by separately developing the plasma and CNS compartments, subsequently linking them into the final model. The plasma compartment was built using estimated plasma PK parameters. The CNS compartment was constructed as a physiologically based model comprising nine distinct compartments, employing relevant CNS physiological parameters. In our updated model (LeiCNS-PK3.2), two key components were newly incorporated: (1) an intracellular conversion process, describing the formation and elimination kinetics of acyclovir and ganciclovir triphosphate metabolites; and (2) active transport across the brain cell membrane, modeled using the AF_{BCM} (Fig. 1).

2.3.1. Drug specific parameters

In our current work, LeiCNS-PK3.2 also requires three types of drug specific parameters including physico-chemical parameters, $K_{p,uu}$ values (for BBB, BCSFB, and Cell), and intracellular drug metabolite formation and elimination parameters (k_{form} and k_{elim}). We obtained drug physiochemical information, including molecular weight, lipophilicity (expressed as logP), and acid/base ionization constants (as pKa and pKb), from DrugBank version 5.1.9. LogP and pKa/pKb values were estimated using the ALOGPS and Chemaxon methods, respectively. We calculated $K_{p,uu,BBB}$ and $Kp_{uu,BCSFB}$ values either using the AUC ratio or by the steady-state concentration ratio between ECF and CSF compartments, respectively, and plasma (Table I). Since human $K_{p,uu,BBB}$ value was unavailable for acyclovir, the rat value was used to calculate its AF_{BBB}. This AF_{BBB} was further adjusted using the ratio of P-glycoprotein (P-gp), organic anion transporters (OATs) and organic cation transporters (OCTs) transporter expression between human and rat (Al-Majdoub, et al., Mol Pharm, 2019; Uchida, et al., J Neurochem, 2011), based on the evidence that acyclovir is a substrate of both transporter families (Yang, et al., Expert Opinion On Drug Metabolism and Toxicology, 2022). These $K_{p,uu,BBB/BCSFB/Cell}$ values were then used to derive the $AF_{ECF/LV/TFV/BCM}$ (Saleh, et al., J Pharmacokinet Pharmacodyn, 2021b), which corrects for active transport processes at the BBB, BCSFB or brain cell membrane in our model (Table I). The intracellular conversion process was incorporated into the LeiCNS-PK3.2 model with these formation and elimination rate constants (k_{form} and k_{elim}) of each triphosphate metabolite (Figure S1).

2.3.2. Plasma PK parameters

Empirical compartmental models were used to describe the plasma PK in rat and human. The plasma PK parameters (Table II) for acyclovir and ganciclovir were estimated using Monolix version 2021R2 (Lixoft, Orsay, France).

2.3.3. CNS system-specific parameters

The CNS physiological parameters for human and rat have been collected and reported in our previous paper (Saleh, et al., J Pharmacokinet Pharmacodyn, 2021a).

2.4. PK data for model validation

Rat and human data (Table III) from multiple CNS compartments were extracted using WebPlotDigitizer version 4.5 (https://automeris.io/WebPlotDigitizer/).

The predictions of both rat and human models by LeiCNS-PK3.2 under the indicated dosing regimens (Table S1) were compared to observed *in vivo* data from various sources (Table S1). The predictive accuracy of LeiCNS-PK3.2 was further assessed using metrics including the squared Pearson correlation coefficient (Pearson R^2), the absolute average fold error (AAFE) across all data points, and the root mean squared error (RMSE).

2.5. PK analysis of brain ECF and intracellular active metabolite concentrations

BrainECF and active metabolite concentrations in brainICF were first simulated under standard dosing regimens (acyclovir: 10 mg/kg, three times daily; ganciclovir: 5 mg/kg, twice daily) for successive 6 doses and at the steady state. The simulated brainECF concentrations of parent drugs were compared to the reported IC_{50} values. To evaluate drug accumulation in the two compartments, the accumulation ratio (R_{ac}) (Li, et al., Curr Drug Metab, 2013) was calculated as the ratio of the area under the concentration–time curve at the steady state ($AUC_{0-\tau,ss}$) to

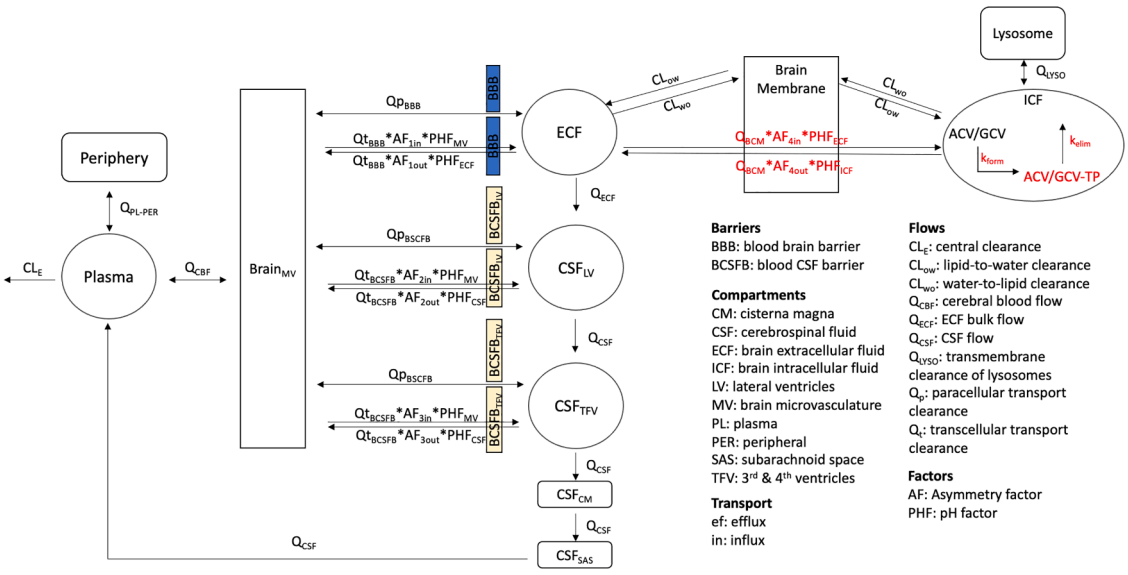

Fig. 1. The model structure of LeiCNS-PK3.2. LeiCNS-PK3.2 builds upon the LeiCNS-PK3.0, which employs an empirical model to represent the systemic circulation and a physiologically based model for key CNS compartments, including brain microvessels (MV), brain parenchyma (*i.e.*, brain extracellular fluid [brainECF], brain intracellular fluid [brainICF], and brain membrane), as well as CSF compartments (*i.e.*, lateral ventricle [LV], third and fourth ventricle [TFV], cisterna magna [CM], and the subarachnoid space [SAS]). In LeiCNS-PK3.2, we extended LeiCNS-PK3.0 to describe active transport on the brain membrane and intracellular conversion from the parent drug to its active triphosphate, by introducing new components (highlighted in red).

Table 1
Drug parameters for active transport.

Parameter	$K_{p,uu,BBB}$	$AF_{in,ECF}$	$AF_{out,ECF}$	$K_{p,uu,BCSFB}$	$AF_{in,LV}$	$AF_{out,LV}$	$AF_{in,TFV}$	$AF_{out,TFV}$	$f_{u,brain}$	$V_{u,brain}$	$K_{p,uu,cell}$	$AF_{in,Cell}$	$AF_{out,Cell}$
Rat													
acyclovir	0.32[a]	1	412.91	0.18[a]	1	7274	1	7336.34	0.37[b]	2.75[b]	1	1	1
ganciclovir	0.16[c]	1	4553.52	0.03[c]	1	228,161.6	1	228,342.8	0.85[d]	1.45[d]	1.23	1.46	1
	0.06[e]	1	14,298.52	0.066[e]	1	99,618.66	1	99,937.62	0.85[d]	1.45[d]	1.23	1.46	1
Human													
acyclovir	0.32[f]	1	34.51	0.26[g]	1	1456.66	1	1469.38	0.37[h]	2.75[h]	1	1	1
ganciclovir	0.77[i]	1	167.18	0.46[i]	1	2631.67	1	2653.38	0.85[h]	1.45[h]	1.23	1.46	1

[a] $K_{p,uu,BBB}$ value was calculated by unbound AUC ratio of brainECF to plasma observed from Sahn et al. (Shan, et al., Eur J Drug MeTable Pharmacokinet, 2022); $K_{p,uu,BCSFB}$ value was calculated using unbound CSF to plasma ratio based on data from Kim et al. (Kim, et al., Pain Physician, 2016).

[b] Values were predicted by the *in silico* model of Kawashima et al. (Kawashima, et al., J Med Chem, 2023).

[c] Values were calculated by unbound AUC ratio of brainECF or CSF to plasma observed from Chen et al. (Chen, et al., Pharmacology Research and Perspectives, 2020).

[d] Value of $f_{u,brain}$ was direct obtained from Lui et al. (Liu, et al., Drug MeTable Dispos, 2009); $V_{u,brain}$ (mL* g^{-1} brain) was calculated using Eq. (1) based on data from Lui et al. (Liu, et al., Drug MeTable Dispos, 2009).

[e] $K_{p,uu,BBB}$ and $K_{p,uu,BCSFB}$ values were calculated by unbound AUC ratio of brainECF to plasma and unbound concentration ratio of CSF to plasma at steady state observed from Lui et al. (Liu, et al., Drug MeTable Dispos, 2009), respectively.

[f] Rat $K_{p,uu,BBB}$ value was input and AF was corrected using the ratio of OAT and OCT expression between humans and rats, divided by 8 since expression levels of these transporters are at least eightfold lower in humans than in rats (Al-Majdoub, et al., Mol Pharm, 2019; Uchida, et al., J Neurochem, 2011).

[g] Value was calculated using the average value of unbound CSF to plasma ratios from Lycke et al. (Lycke, et al., Antimicrob Agents Chemother, 2003; Smith, et al., Antimicrobial Agents and Chemotherapy, 2010).

[h] Assumed to be the same as in rat.

[i] $K_{p,uu,BBB}$ value were calculated by unbound AUC ratio of brainECF to plasma at steady state from Peredo et al. (Peredo, et al., BMJ Case Rep, 2015); $K_{p,uu,BCSFB}$ value and unbound concentration ratio of CSF to plasma at steady state observed from Fletcher et al. (Fletcher, et al., Clinical Pharmacology and Therapeutics, 1986).

that following the first dose ($AUC_{0-\tau,1}$). To further compare the time to steady state between drug in brainECF and intracellular active metabolite TP in brainICF, the predicted concentrations were normalized by the average steady state concentrations per dosing interval.

2.6. Sensitivity analysis

2.6.1. Effects of pathological changes in physiological parameters on target-site concentrations

Since physiological parameters may change due to the CNS pathologies, we conducted a sensitivity analysis to compare intracellular PK predictions of TP metabolites between healthy and diseased values of relevant parameters. Pathological changes associated with CNS viral encephalitis were considered to include a 2-fold range increase in the BBB pore size (Pouplin, et al., Antimicrob Agents Chemother, 2011), a 2-fold range increase in SAS volume (Djukic, et al., J Neuroinflammation, 2022; Johanson, et al., Cerebrospinal Fluid Research, 2008), and a 4-fold increase CSF flow rate (Bauer, et al., Child's Nervous System: ChNS: Official Journal of the International Society For Pediatric Neurosurgery, 2008; Tariq, et al., Acta Neurochirurgica, 2023). Simulations were performed under standard dosing regimens (acyclovir: 10 mg/kg, three times daily; ganciclovir: 5 mg/kg, twice daily), applying either healthy human physiological parameters or modified parameters reflecting reported pathological conditions.

Table 2
Plasma parameters of acyclovir and ganciclovir in rats and human.

Parameter	Acyclovir		Ganciclovir		
	Rat[a]	Human[b]	Rat[c]	Rat[d]	Human[e]
CL_{Cen}/F (mL* min^{-1})	3.9	917	4.5	9.6	532
$Q_{Cen\text{-}Peri1}/F$ (mL* min^{-1})	2.2	NA	NA	NA	342
V_{Cen}/F (mL)	110	176,745	311	180	75,374
V_{Peri1}/F (mL)	106	NA	NA	NA	101,427
K_a (min^{-1})	NA	0.025	NA	NA	0.013
T_{lag} (min^{-1})	NA	51	NA	NA	52.9
F (%)	NA	54.5[f]	NA	100	60[g]

[a] Parameter values were estimated based on plasma data from (Shan, et al., Eur J Drug MeTable Pharmacokinet, 2022).
[b] Parameter values were estimated based on plasma data from 1000 mg (Lycke, et al., Antimicrob Agents Chemother, 2003) and 2000 mg of valacyclovir (Smith, et al., Antimicrob Agents Chemother, 2010).
[c] Parameter values are estimated based on plasma data from (Chen, et al., Pharmacology Research and Perspectives, 2020).
[d] Parameter values were estimated based on plasma data from (Liu, et al., Drug MeTable Dispos, 2009).
[e] Parameter values were estimated based on plasma data from (Peredo, et al., BMJ Case Rep, 2015).
[f] Value was derived from (Soul-Lawton, et al., Antimicrob Agents Chemother, 1995).
[g] Value was derived from (Pescovitz, et al., Antimicrob Agents Chemother, 2000).

2.6.2. *Effects of $k_{p,uu,cell}$ values on target-site concentrations*

Using rat-derived $K_{p,uu,cell}$ values directly for human predictions might introduce a bias in PK prediction. To assess the impact of variations in $K_{p,uu,cell}$ on PK predictions for intracellular TPs, we performed a series of simulations using the LeiCNS-PK3.2 human model. The standard acyclovir/ganciclovir dosing regimens described above were applied, varying the $K_{p,uu,cell}$ values by 2-, 3-, and 4-fold relative to the original rat-derived values. All other model parameters remained fixed, and CNS physiological parameters were set to reflect healthy human conditions.

3. Results

3.1. *Model predictions vs. observations*

The LeiCNS-PK3.2 model showed good predictive accuracy for plasma, brainECF, and SAS compartments, with simulated PK profiles of acyclovir and ganciclovir closely matching most observed data from different sources (Figure S1). We further assessed the correlation between the observed and model-simulated concentrations of acyclovir and ganciclovir using multiple metrics. The simulations fell within a 2-fold prediction error range, with high correlation coefficients (R^2), indicating strong predictive performance. Additionally, low absolute average fold error (AAFE) and root mean square error (RMSE) values were observed across both species (Fig. 2).

3.2. *Comparative PK analysis on brainECF parent drugs and brainICF active metabolites*

Simulated concentrations of acyclovir and ganciclovir in brainECF fluctuated around their IC_{50} values, and trough concentrations (C_{min}) values often fell below the IC_{50} (Fig. 3A). In contrast, intracellular triphosphate metabolites (acyclovir-TP and ganciclovir-TP) concentrations in brainICF gradually increased over six successive doses (Fig. 3A). Direct comparison with experimentally observed intracellular concentrations or intracellular IC_{50} values was not possible, as such data are unavailable for these metabolites. To further compare PK differences between parent drugs in brainECF and intracellular active metabolites in brainICF, we analyzed the drug accumulation ratio $AUC_{0-\tau,ss}$ / $AUC_{0-\tau,1}$ (Fig. 3B) as well as the time to reach steady state (Fig. 3C).

The simulations indicated markedly greater accumulation of acyclovir-TP and ganciclovir-TP in brainICF than of their parent drugs in brainECF. While brainECF concentrations reached steady state rapidly after the first dosing interval, intracellular metabolite concentrations increased gradually and did not attain steady-state levels even after six consecutive doses.

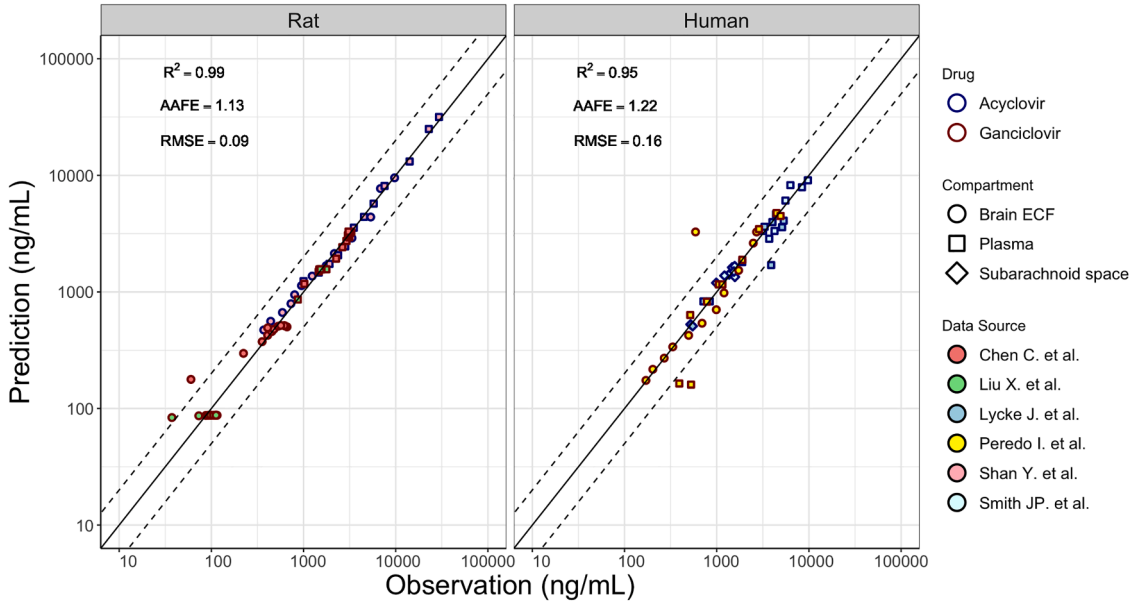

Fig. 2. Observed *vs.* predicted concentrations of acyclovir and ganciclovir in rat and human models. The correlation between observed and model-simulated concentrations of acyclovir and ganciclovir is shown for rat (left panel) and human (right panel) datasets. Observations include acyclovir and ganciclovir data from plasma, brain extracellular fluid (brainECF), and the subarachnoid space. Symbols represent different compartments, while outliers are highlighted by color (blue for acyclovir, red for ganciclovir). Data sources from literature are highlighted in the legend. Solid diagonal lines represent the perfect agreement, and dashed lines indicate a 2-fold prediction error. Model performance metrics, including the coefficient of determination (R^2), average absolute fold error (AAFE), and root mean square error (RMSE), are shown within each panel.

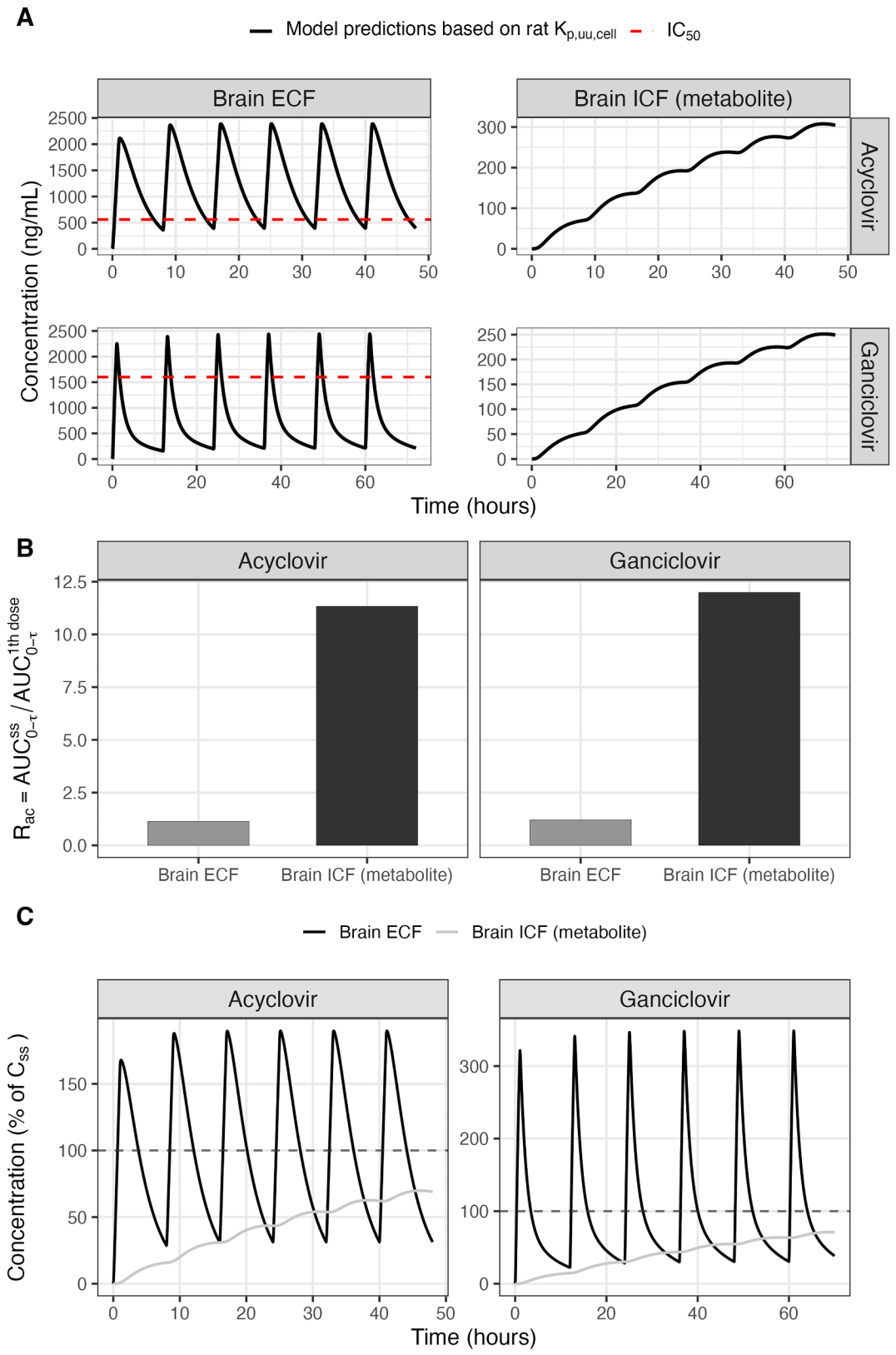

Fig. 3. Simulation-based pharmacokinetic comparison of acyclovir and ganciclovir in brain extracellular fluid (ECF) and their active triphosphate metabolites in brain intracellular fluid (brainICF) under standard dosing regimens (Acyclovir: 10 mg/kg, three times daily; Ganciclovir: 5 mg/kg, twice daily). Panel A showed predicted concentration–time profiles of acyclovir and ganciclovir in brainECF and their respective triphosphate metabolites in brainICF. Red dashed lines indicate the reported IC_{50} values. Panel B showed accumulation ratios ($R_{ac} = AUC_{0-\tau,ss} / AUC_{0-\tau,1}$) calculated for brainECF (parent drugs) and brainICF (active metabolites), illustrating the extent of parent drug and active metabolite accumulation relative to the first dosing interval. Panel C compared the time to reach steady-state concentrations, depicted by normalizing predicted concentrations to their average steady-state concentrations ($C_{ss,average}$) per dosing interval.

3.3. Effect of encephalitic pathology and $k_{p,uu,cell}$ value on active triphosphate brainICF PK

When we shifted from healthy (perturbation = 1) to pathological values for pore size of the blood-brain barrier (1< perturbation ≤ 2), volume of SAS (1< perturbation ≤2), and CSF flow rate (1< perturbation ≤4), the TP PK profiles in brainICF remained essentially unchanged (Fig. 4). Because directly using rat $K_{p,uu,cell}$ values as input to our human model could introduce bias, we also tested a two-fold range of $K_{p,uu,cell}$ values. These simulations showed that increasing $K_{p,uu,cell}$ led to proportional increases in active-metabolite exposure.

4. Discussion

Direct measurement of intracellular triphosphate metabolite concentrations in human CNS remains technically infeasible, creating a critical knowledge gap in understanding target-site PK profiles of antiviral nucleoside analog for CNS infections. This study presents the LeiCNS-PK3.2 model as a tool to predict intracellular concentrations of the active triphosphate metabolites of acyclovir and ganciclovir in the CNS. Our simulations revealed distinct PK profile differences between parent drugs in brainECF and their metabolites in brainICF.

LeiCNS-PK3.2 is an improved version of the previous LeiCNS-PK1.0 (Yamamoto, et al., CPT Pharmacometrics Syst Pharmacol, 2017) and 3.0 frameworks (Saleh, et al., J Pharmacokinet Pharmacodyn, 2021b). The earlier two models described only passive diffusion between brainECF and brainICF spaces. Similar to LeiCNS-PK1.0 (Yamamoto, et al., CPT Pharmacometrics Syst Pharmacol, 2017), where active transport across the BBB and BCSFB was incorporated through $K_{p,uu,BBB}$ and $K_{p,uu,BCSFB}$, LeiCNS-PK3.2 extends this concept by integrating active transport across brain cell membranes using AF derived from $K_{p,uu,cell}$, thereby accounting for net influx/efflux mediated by active transporter on brain parenchymal cells. Assuming the presence of only passive exchange might overlook the additional transporter-dependent barrier between brainECF and brainICF, as evidenced by *in vivo* observations confirming active transport roles for P-gp or OATs at brain parenchymal level (Kervezee, et al., Aaps j, 2014; Scism, et al., Brain Res, 2000; Syvänen, et al., Aaps j, 2012). Furthermore, LeiCNS-PK3.2 introduced intracellular metabolite kinetics by explicitly modelling the intracellular formation and elimination of TP metabolites via a first-order kinetic module. This approach was performed earlier for other nucleoside analogs such as remdesivir and molnupiravir (Saleh, et al., Eur J Pharm Sci, 2023). LeiCNS-PK3.2 offers a more comprehensive representation by incorporating mechanisms such as active transport and intracellular conversion within brain cells. Although the lack of intracellular concentration data currently restricts direct validation and comparison of model performance between version 3.0 and the present model, this framework enables a deeper mechanistic understanding of local drug exposure within the CNS. Importantly, LeiCNS-PK3.2 can predict the impact of physio-pathological changes in BBB permeability, CSF flow, and SAS volume on intracellular TP exposure. The simulations demonstrated that such changes had minimal influence on brainICF triphosphate exposure.

In our modeling framework, acyclovir and ganciclovir in brainICF

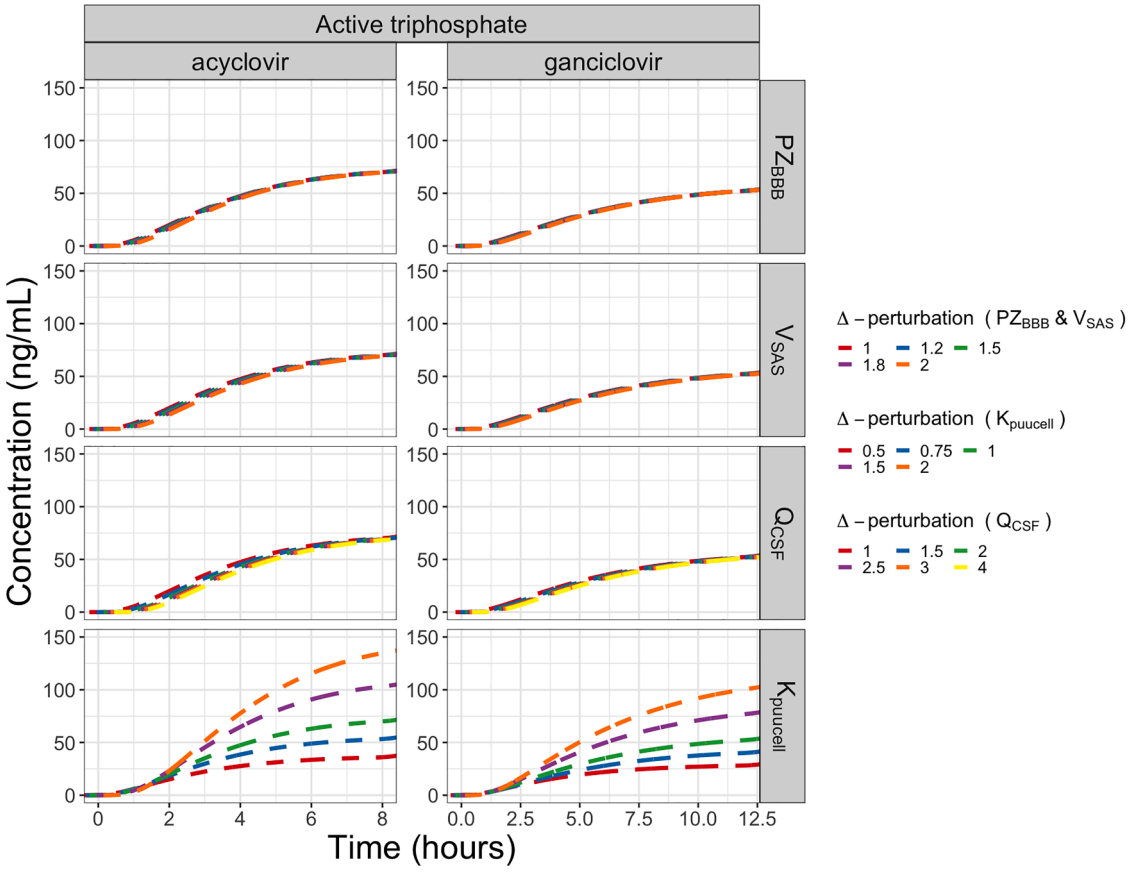

Fig. 4. Sensitivity analysis of intracellular active metabolite pharmacokinetics (PK) in brain intracellular fluid (brainICF). Concentration–time profiles of acyclovir triphosphate (left column) and ganciclovir-triphosphate (right column) are shown, as predicted over one dosing interval (0–8 h for acyclovir; 0–12 h for ganciclovir) under standard regimens (acyclovir: 10 mg/kg, three times daily; ganciclovir: 5 mg/kg, twice daily). From top to bottom, each row shows the effect of progressively increasing (Δ) one model parameter to mimic pathological changes: BBB pore size (PZ_{BBB}; Δ = 1, 1.2, 1.5, 1.8, 2), subarachnoid space volume (V_{SAS}; Δ = 1, 1.2, 1.5, 1.8, 2), CSF flow rate (Q_{CSF}; Δ = 1, 1.5, 2, 2.5, 3, 4), and cellular unbound partition coefficient ($K_{p,uu,cell}$; Δ = 0.5, 0.75, 1, 1.5, 2). Colored lines represent fold changes on relevant parameters including PZ_{BBB}, V_{SAS}, Q_{CSF}, and $K_{p,uu,cell}$.

were assumed to be instantly converted to their triphosphate forms. This assumption aligns with previous successful PBPK modeling practices that adopted a similar simplification to characterize the intracellular drug conversion, owing to the very low intracellular concentrations of intermediate phosphorylated drugs observed *in vitro* (Hughes, et al., CPT: Pharmacometrics and Systems Pharmacology, 2020; Saleh, et al., European Journal of Pharmaceutical Sciences: Official Journal of the European Federation For Pharmaceutical Sciences, 2023; Tanaudommongkon, et al., Br J Clin Pharmacol, 2022). Additionally, a linear process was assumed for the phosphorylation step of converting acyclovir/ganciclovir into acyclovir/ganciclovir-TP, which was justified by the low intracellular acyclovir and ganciclovir levels relative to the K_m values for viral kinases (Black, et al., Proceedings of the National Academy of Sciences of the United States of America, 1996; Kokoris, et al., Protein Sci, 2002). In LeiCNS-PK3.2 model, the step of drug conversion into their active metabolites was only modeled within the brainICF given the fact that during the HSV and HCMV encephalitis the viruses primarily infected the CNS instead of the circulation system (Solomon, et al., Pract Neurol, 2007). In the sites with lower or no viral infection, normal cellular enzymes predominantly catalyze the intracellular conversion but with much lower efficiency compared to viral kinases. The active metabolites concentrations are thereby considered minimal in the system. Also given the relatively large molecular weight (~500 Da) of acyclovir/ganciclovir-TP, these metabolites might have limited permeability across the BBB, which restricts their significant pharmacologically amount in the CNS (Pardridge, NeuroRx, 2005).

In LeiCNS3.2, rat-derived $K_{p,uu,cell}$ values were incorporated into the human model due to the absence of human data. In rats, ganciclovir showed higher $K_{p,uu,cell}$ values, suggesting dominant active influx transport, whereas predicted $K_{p,uu,cell}$ value for acyclovir was equal to 1 suggesting that passive diffusion is the dominant mechanism. Species-specific differences in transporter expression and cellular uptake might fluence $K_{p,uu,cell}$ values for acyclovir and ganciclovir. Here, $K_{p,uu,cell}$ was calculated as the product of $f_{u,brain}$ (representing non-specific binding to the brain membrane lipid) and $V_{u,brain}$ (capturing the extent of intracellular drug distribution into brain cells) (Loryan, et al., Pharm Res, 2014). Although $f_{u,brain}$ value of an individual drug tends to be similar across mammalian species (Di, et al., Drug MeTable Dispos, 2011), the value itself could be affected by aging and disease conditions since the lipid content and composition change with age or pathological conditions (Eddy, et al., J Gerontol, 1975; Martínez-Gardeazabal, et al., Biochim Biophys Acta Biomembr, 2017; Zhang, et al., Neurobiol Aging, 1996). The values of $V_{u,brain}$, which represent the drug's overall extra-intracellular distribution influenced by pH partitioning and active transport (Fridén, et al., Drug MeTable Dispos, 2009) and while pH values in brainECF and brainICF can be considered very similar between species (Chesler, Physiol Rev, 2003), active transport functionalities may vary across species. Although existing data on $V_{u,brain}$ have largely been generated in rodent models (Loryan, et al., Pharmaceutical Research, 2022) and show consistency between rat and mouse (Loryan, et al., Fluids and Barriers of the CNS, 2013), it is plausible that $V_{u,brain}$ differs significantly between rodent and human brains due to the species-specific difference in the active transporter expression on brain cell membrane. Rats, for instance, have exhibited different transporter expression levels at least at CNS barriers compared to humans (Uchida, et al., J Neurochem, 2011). Due to the limited availability of human-specific data on human $K_{p,uu,cell}$, the human model directly used the rat-derived as input, and therefore introduce uncertainty into our predictions. Future work on measuring human $K_{p,uu,cell}$ by *in vitro* or *in vivo* model system should be performed to refine our CNS PBPK model.

Our simulations highlighted a PK disconnect between parent drug in brain ECF and it's active TP in brain ICF for both acyclovir and ganciclovir. Since evaluating efficacy of acyclovir and ganciclovir is based on parent drug concentration rather than their TP, the PK disparity can lead to different conclusions: intracellular accumulation of TPs may sustain pharmacologically relevant levels even after brainECF concentrations of the parent drugs decline below PK/PD target thresholds. Mechanistically, brainICF concentrations of acyclovir-TP and ganciclovir-TP are the most relevant drivers of antiviral activity and relying on parent drug levels in plasma or brainECF as surrogates may therefore underestimate the true drug effect. Our PK findings are consistent with the general principle that most active metabolites of nucleoside analogues rarely eliminate faster than their parent drugs (Rayner, et al., Clin Pharmacol Ther, 2021). Notably, Furman et al. (Furman, et al., Antimicrob Agents Chemother, 1981) reported a much shorter half-life for acyclovir-TP (1–2 h) compared to the ~27 h reported by Sauer et al. (Sauer, et al., Antiviral Res, 2020), while only the latter value was applied in the LeiCNS-PK3.2 model. This discrepancy likely arises from concentration-dependent elimination kinetics of TPs via viral polymerase. Furman et al. observed a biphasic acyclovir-TP decline where high initial 100 μM acyclovir exposure saturated polymerase ($C_{TP} >> K_m$), driving maximal incorporation (V_{max}) into viral DNA and resulting in a rapid absolute elimination rate during the initial phase, followed by slower decline as concentrations fell. In contrast, Sauer et al.'s lower 5 μM concentration drove a lower elimination rate and a longer terminal half-life. The applied lower concentration might be closer to the *in vivo* situation due to closely matching predicted brain ECF levels by LeiCNS-PK3.2. Overall, simulations highlight the need to explicitly model intracellular TP kinetics for accurate antiviral assessment of nucleoside analogues.

Several limitations of our modeling should be acknowledged. First, the intracellular conversion process of active metabolite was incorporated using *in vitro* data obtained from non-neuronal cell lines rather than brain cells. Moreover, in the HSV infection *in vitro* system, acyclovir was added into the culture medium only one hour after viral inoculation, which might be insufficient for viral enzyme production to initiate the phosphorylation steps (Harkness, et al., J Virol, 2014). Consequently, the onset of acyclovir-TP formation was delayed during the early phase of incubation (Sauer, et al., Antiviral Res, 2020), unlike the *in vivo* CNS settings where viral enzymes might be already present at the time of drug exposure. Second, the lack of human CNS intracellular TP data prevented direct validation of our simulated TP concentrations, limiting the confirmation of the model's predictive accuracy. Finally, the lack of established PK/PD index built on TP kinetics hinders the further antiviral efficacy evaluation. Despite these limitations, LeiCNS-PK3.2 provides a framework to evaluate nucleoside analog drug TP level at the CNS target site (brainICF) and to analyze the potential PK disparity in parallel with non-target compartments such as brainECF. Future work should focus on quantifying active metabolite exposures in infected brain cells or tissues. Optimizing *in vitro* infection model, for example by extending the acyclovir addition time from 1 h (commonly used *in vitro*) to 2–3 h post-infection, might improve relevance to the *in vivo* situation. In addition, integrating intracellular TP kinetics with viral dynamic modeling will be essential to define relevant PK/PD targets and to support model-informed optimization of nucleoside analog dosing for CNS infections.

5. Conclusion

In summary, LeiCNS-PK3.2 provides a mechanistic framework for predicting intracellular triphosphate exposure of antiviral drugs in the CNS. Our simulated results revealed that brain ECF concentrations were not ideal surrogates for intracellular active metabolite levels. Future work should determine human-specific $Kp_{,uu,cell}$ values and establish intracellular PK/PD targets to optimize CNS antiviral dosing.

CRediT authorship contribution statement

Ming Sun: Writing – review & editing, Writing – original draft, Visualization, Validation, Software, Methodology, Investigation, Formal analysis, Data curation. **Martijn L. Manson:** Writing – review & editing, Supervision. **Tingjie Guo:** Writing – review & editing, Supervision,

Methodology, Investigation, Formal analysis. **Elizabeth C.M. de Lange:** Writing – review & editing, Validation, Supervision, Resources, Project administration, Methodology, Conceptualization.

Supplementary materials

Supplementary material associated with this article can be found, in the online version, at doi:10.1016/j.ejps.2026.107496.

Data availability

Data will be made available on request.

References

Al-Majdoub, Z.M., Al Feteisi, H., Achour, B., Warwood, S., Neuhoff, S., Rostami-Hodjegan, A., Barber, J., 2019. Proteomic quantification of Human blood-brain barrier SLC and ABC transporters in healthy individuals and dementia patients. Mol. Pharm. 16, 1220–1233.

Angello, J.C., Pendergrass, W.R., Norwood, T.H., Prothero, J., 1987. Proliferative potential of human fibroblasts: an inverse dependence on cell size. J. Cell Physiol. 132, 125–130.

Bällgren, F., Svane, N., Ginosyan, A., Pedersen, A.B.V., Li, S., Mahajan, J., Nielsen, M.S., Brodin, B., Loryan, I., 2025. Comparative analysis of the uptake of the H(+)/OC antiporter substrate oxycodone across and into brain endothelial and parenchymal cells with in vitro-in vivo extrapolation. Fluids. Barriers. CNS. 22, 109.

Bauer, D.F., Tubbs, R.S., Acakpo-Satchivi, L., 2008. Mycoplasma meningitis resulting in increased production of cerebrospinal fluid: case report and review of the literature. Child's Nerv. Syst.: ChNS: Off. J. Int. Soc. Pediatr. Neurosurg. 24, 859–862.

Black, M.E., Newcomb, T.G., Wilson, H.M., Loeb, L.A., 1996. Creation of drug-specific herpes simplex virus type 1 thymidine kinase mutants for gene therapy. Proc Natl. Acad. Sci. USA 93, 3525–3529.

Chen, C., Zhou, H., Guan, C., Zhang, H., Li, Y., Jiang, X., Dong, Z., Tao, Y., Du, J., Wang, S., Zhang, T., Du, N., Guo, J., Wu, Y., Song, Z., Luan, H., Wang, Y., Du, H., Zhang, S., Li, C., Chang, H., Wang, T., 2020. Applicability of free drug hypothesis to drugs with good membrane permeability that are not efflux transporter substrates: a microdialysis study in rats. Pharmacol. Res. Perspect. 8, e00575.

Chesler, M., 2003. Regulation and modulation of pH in the brain. Physiol. Rev. 83, 1183–1221.

CJ, B., CR, H., FA, M., 2017. Pathogenesis of virus infections. Fenner White's Med. Virol.

da Silva, M.B., Costa, V.M.A., Pereira, V.R.A., de Albertim, G.J.B., de Melo, E.B.B., Bezerra, D.P., da Silva, R.P., Rodrigues, C.G., Carneiro, C.M.M., Yuldasheva, L.N., Krasilnikov, O.V., 2010. Ion channels in volume regulation of clonal kidney cells. Cell Prolif. 43, 529–541.

de Lange, E.C., 2013. The mastermind approach to CNS drug therapy: translational prediction of human brain distribution, target site kinetics, and therapeutic effects. Fluids. Barriers. CNS. 10, 12.

de Lange, E.C.M., Hammarlund Udenaes, M., 2022. Understanding the blood-brain barrier and beyond: challenges and opportunities for novel CNS therapeutics. Clin. Pharmacol. Ther. 111, 758–773.

Di, L., Umland, J.P., Chang, G., Huang, Y., Lin, Z., Scott, D.O., Troutman, M.D., Liston, T. E., 2011. Species independence in brain tissue binding using brain homogenates. Drug Metab. Dispos. 39, 1270–1277.

Djukic, M., Lange, P., Erbguth, F., Nau, R., 2022. Spatial and temporal variation of routine parameters: pitfalls in the cerebrospinal fluid analysis in central nervous system infections. J. Neuroinflammation. 19, 174.

Eddy, D.E., Harman, D., 1975. Rat brain fatty acid composition: effect of dietary fat and age. J. Gerontol. 30, 647–654.

Fletcher, C., Sawchuk, R., Chinnock, B., de Miranda, P., Balfour, H.H., 1986. Human pharmacokinetics of the antiviral drug DHPG. Clin. Pharmacol. Ther. 40, 281–286.

Fridén, M., Ducrozet, F., Middleton, B., Antonsson, M., Bredberg, U., Hammarlund-Udenaes, M., 2009. Development of a high-throughput brain slice method for studying drug distribution in the central nervous system. Drug Metab. Dispos. 37, 1226–1233.

Furman, P.A., de Miranda, P., St Clair, M.H., Elion, G.B., 1981. Metabolism of acyclovir in virus-infected and uninfected cells. Antimicrob. Agents Chemother. 20, 518–524.

Gentry, B.G., Drach, J.C., 2014. Metabolism of cyclopropavir and ganciclovir in human cytomegalovirus-infected cells. Antimicrob. Agents Chemother. 58, 2329–2333.

Hammarlund-Udenaes, M., Fridén, M., Syvänen, S., Gupta, A., 2008. On the rate and extent of drug delivery to the brain. Pharm. Res. 25, 1737–1750.

Harkness, J.M., Kader, M., DeLuca, N.A., 2014. Transcription of the herpes simplex virus 1 genome during productive and quiescent infection of neuronal and nonneuronal cells. J. Virol. 88, 6847–6861.

Hughes, J.H., Sweeney, K., Ahadieh, S., Ouellet, D., 2020. Predictions of systemic, intracellular, and lung concentrations of azithromycin with different dosing regimens used in COVID-19 clinical trials. CPT Pharmacomet. Syst. Pharmacol. 9, 435–443.

Johanson, C.E., Duncan, J.A., Klinge, P.M., Brinker, T., Stopa, E.G., Silverberg, G.D., 2008. Multiplicity of cerebrospinal fluid functions: new challenges in health and disease. CerebroSpinal Fluid. Res. 5, 10.

Kawashima, H., Watanabe, R., Esaki, T., Kuroda, M., Nagao, C., Natsume-Kitatani, Y., Ohashi, R., Komura, H., Mizuguchi, K., 2023. DruMAP: a novel drug metabolism and pharmacokinetics analysis platform. J. Med. Chem. 66, 9697–9709.

Kervezee, L., Hartman, R., van den Berg, D.J., Shimizu, S., Emoto-Yamamoto, Y., Meijer, J.H., de Lange, E.C., 2014. Diurnal variation in P-glycoprotein-mediated transport and cerebrospinal fluid turnover in the brain. AAPS. J. 16, 1029–1037.

Khor, S.P., Bozigian, H., Mayersohn, M., 1991. Potential error in the measurement of tissue to blood distribution coefficients in physiological pharmacokinetic modeling. Residual tissue blood. II. Distribution of phencyclidine in the rat. Drug Metab. Dispos. 19, 486–490.

Kim, J.H., Lee, M.K., Kim, J.E., Kim, S.H., Choi, S.S., 2016. Comparison of intrathecal concentrations of acyclovir following epidural and intravenous administration in rats. Pain. Physician 19, E613–E619.

Kokoris, M.S., Black, M.E., 2002. Characterization of herpes simplex virus type 1 thymidine kinase mutants engineered for improved ganciclovir or acyclovir activity. Protein Sci. 11, 2267–2272.

Lee, G., Dallas, S., Hong, M., Bendayan, R., 2001. Drug transporters in the central nervous system: brain barriers and brain parenchyma considerations. Pharmacol. Rev. 53, 569–596.

Li, L., Li, X., Xu, L., Sheng, Y., Huang, J., Zheng, Q., 2013. Systematic evaluation of dose accumulation studies in clinical pharmacokinetics. Curr. Drug Metab. 14, 605–615.

Liu, X., Van Natta, K., Yeo, H., Vilenski, O., Weller, P.E., Worboys, P.D., Monshouwer, M., 2009. Unbound drug concentration in brain homogenate and cerebral spinal fluid at steady state as a surrogate for unbound concentration in brain interstitial fluid. Drug Metab. Dispos. 37, 787–793.

Loryan, I., Fridén, M., Hammarlund-Udenaes, M., 2013. The brain slice method for studying drug distribution in the CNS. Fluids. Barriers. CNS. 10, 6.

Loryan, I., Reichel, A., Feng, B., Bundgaard, C., Shaffer, C., Kalvass, C., Bednarczyk, D., Morrison, D., Lesuisse, D., Hoppe, E., Terstappen, G.C., Fischer, H., Di, L., Colclough, N., Summerfield, S., Buckley, S.T., Maurer, T.S., Fridén, M., 2022a. Unbound brain-to-plasma partition coefficient, K(p,uu,brain)-a game changing parameter for CNS drug discovery and development. Pharm. Res. 39, 1321–1341.

Loryan, I., Reichel, A., Feng, B., Bundgaard, C., Shaffer, C., Kalvass, C., Bednarczyk, D., Morrison, D., Lesuisse, D., Hoppe, E., Terstappen, G.C., Fischer, H., Di, L., Colclough, N., Summerfield, S., Buckley, S.T., Maurer, T.S., Fridén, M., 2022b. Unbound brain-to-plasma partition coefficient, kp,uu,brain—a game changing parameter for CNS drug discovery and development. Pharm. Res. 39, 1321–1341.

Loryan, I., Sinha, V., Mackie, C., Van Peer, A., Drinkenburg, W., Vermeulen, A., Morrison, D., Monshouwer, M., Heald, D., Hammarlund-Udenaes, M., 2014. Mechanistic understanding of brain drug disposition to optimize the selection of potential neurotherapeutics in drug discovery. Pharm. Res. 31, 2203–2219.

Lycke, J., Malmeström, C., Ståhle, L., 2003. Acyclovir levels in serum and cerebrospinal fluid after oral administration of valacyclovir. Antimicrob. Agents Chemother. 47, 2438–2441.

Martínez-Gardeazabal, J., González de San Román, E., Moreno-Rodríguez, M., Llorente-Ovejero, A., Manuel, I., Rodríguez-Puertas, R., 2017. Lipid mapping of the rat brain for models of disease. Biochim. Biophys. Acta Biomembr. 1859, 1548–1557.

Pardridge, W.M., 2005. The blood-brain barrier: bottleneck in brain drug development. NeuroRx 2, 3–14.

Peredo, I., Helldén, A., Wolmer-Solberg, N., Pohanka, A., Stragliotto, G., Rahbar, A., Ståhle, L., Bellander, B.-M., Söderberg-Nauclér, C., 2015. Ganciclovir concentrations in the cerebral extracellular space after valganciclovir treatment; a case study. BMJ Case Rep. 2015.

Pertinez, H., Rajoli, R.K.R., Khoo, S.H., Owen, A., 2021. Pharmacokinetic modelling to estimate intracellular favipiravir ribofuranosyl-5′-triphosphate exposure to support posology for SARS-CoV-2. J. Antimicrob. Chemother 76, 2121–2128.

Pescovitz, M.D., Rabkin, J., Merion, R.M., Paya, C.V., Pirsch, J., Freeman, R.B., O'Grady, J., Robinson, C., To, Z., Wren, K., Banken, L., Buhles, W., Brown, F., 2000. Valganciclovir results in improved oral absorption of ganciclovir in liver transplant recipients. Antimicrob. Agents Chemother. 44, 2811–2815.

Pouplin, T., Pouplin, J.N., Van Toi, P., Lindegardh, N., Rogier van Doorn, H., Hien, T.T., Farrar, J., Török, M.E., Chau, T.T.H., 2011. Valacyclovir for herpes simplex encephalitis. Antimicrob. Agents Chemother. 55, 3624–3626.

Rayner, C.R., Smith, P.F., Andes, D., Andrews, K., Derendorf, H., Friberg, L.E., Hanna, D., Lepak, A., Mills, E., Polasek, T.M., Roberts, J.A., Schuck, V., Shelton, M.J., Wesche, D., Rowland-Yeo, K., 2021. Model-informed drug development for anti-infectives: state of the art and future. Clin. Pharmacol. Ther. 109, 867–891.

Saleh, M.A.A., Hirasawa, M., Sun, M., Gülave, B., Elassaiss-Schaap, J., de Lange, E.C.M., 2023a. The PBPK LeiCNS-PK3.0 framework predicts Nirmatrelvir (but not Remdesivir or Molnupiravir) to achieve effective concentrations against SARS-CoV-2 in human brain cells. Eur J. Pharm Sci. Off J. Eur. Fed. Pharm Sci. 181, 106345.

Saleh, M.A.A., Hirasawa, M., Sun, M., Gülave, B., Elassaiss-Schaap, J., de Lange, E.C.M., 2023b. The PBPK LeiCNS-PK3.0 framework predicts Nirmatrelvir (but not Remdesivir or Molnupiravir) to achieve effective concentrations against SARS-CoV-2 in human brain cells. Eur. J. Pharm. Sci. 181, 106345.

Saleh, M.A.A., Loo, C.F., Elassaiss-Schaap, J., De Lange, E.C.M., 2021a. Lumbar cerebrospinal fluid-to-brain extracellular fluid surrogacy is context-specific: insights from LeiCNS-PK3.0 simulations. J. Pharmacokinet. Pharmacodyn. 48, 725–741.

Saleh, M.A.A., Loo, C.F., Elassaiss-Schaap, J., De Lange, E.C.M., 2021b. Lumbar cerebrospinal fluid-to-brain extracellular fluid surrogacy is context-specific: insights from LeiCNS-PK3.0 simulations. J. Pharmacokinet. Pharmacodyn. 48, 725–741.

Sauer, H.E., Nguyen, M.L., Williams, J.D., Bowlin, T.L., Gentry, B.G., 2020. Biosynthesis and half-life of MBX-2168-triphosphate in herpes virus-infected cells. Antivir. Res. 175, 104713.

Scism, J.L., Powers, K.M., Artru, A.A., Lewis, L., Shen, D.D., 2000. Probenecid-inhibitable efflux transport of valproic acid in the brain parenchymal cells of rabbits: a microdialysis study. Brain Res. 884, 77–86.

Shan, Y., Cen, Y., Zhang, Y., Tan, R., Zhao, J., Nie, Z., Zhang, J., Yu, S., 2022. Acyclovir brain disposition: interactions with P-gp, bcrp, Mrp2, and Oat3 at the blood-brain barrier. Eur. J. Drug Metab. Pharmacokinet. 47, 279–289.

Smith, J.P., Weller, S., Johnson, B., Nicotera, J., Luther, J.M., Haas, D.W., 2010a. Pharmacokinetics of acyclovir and its metabolites in cerebrospinal fluid and systemic circulation after administration of high-dose valacyclovir in subjects with normal and impaired renal function. Antimicrob. Agents Chemother. 54, 1146–1151.

Smith, J.P., Weller, S., Johnson, B., Nicotera, J., Luther, J.M., Haas, D.W., 2010b. Pharmacokinetics of acyclovir and its metabolites in cerebrospinal fluid and systemic circulation after administration of high-dose valacyclovir in subjects with normal and impaired renal function. Antimicrob. Agents Chemother. 54, 1146–1151.

Solomon, T., Hart, I.J., Beeching, N.J., 2007. Viral encephalitis: a clinician's guide. Pr. Neurol. 7, 288–305.

Soul-Lawton, J., Seaber, E., On, N., Wootton, R., Rolan, P., Posner, J., 1995. Absolute bioavailability and metabolic disposition of valaciclovir, the L-valyl ester of acyclovir, following oral administration to humans. Antimicrob. Agents Chemother. 39, 2759–2764.

Sun, M., Manson, M.L., Guo, T., de Lange, E.C.M., 2024. CNS viral infections-what to consider for improving drug treatment: a plea for using mathematical modeling approaches. CNS. Drugs 38, 349–373.

Sun, M., Manson, M.L., Märtson, A.-G., Bodilsen, J., de Lange, E.C.M., Guo, T., 2025. Revisiting acyclovir dosing for adult viral encephalitis using a full bayesian LeiCNS PBPK modeling approach. Clin. Pharmacokinet.

Syvänen, S., Schenke, M., van den Berg, D.J., Voskuyl, R.A., de Lange, E.C., 2012. Alteration in P-glycoprotein functionality affects intrabrain distribution of quinidine more than brain entry-a study in rats subjected to status epilepticus by kainate. AAPS. J. 14, 87–96.

Tanaudommongkon, A., Chaturvedula, A., Hendrix, C.W., Fuchs, E.J., Shieh, E., Bakshi, R.P., Marzinke, M.A., 2022. Population pharmacokinetics of tenofovir, emtricitabine and intracellular metabolites in transgender women. Br. J. Clin. Pharmacol. 88, 3674–3682.

Tariq, K., Toma, A., Khawari, S., Amarouche, M., Elborady, M.A., Thorne, L., Watkins, L., 2023. Cerebrospinal fluid production rate in various pathological conditions: a preliminary study. Acta Neurochir. 165, 2309–2319.

Uchida, Y., Ohtsuki, S., Katsukura, Y., Ikeda, C., Suzuki, T., Kamiie, J., Terasaki, T., 2011. Quantitative targeted absolute proteomics of human blood-brain barrier transporters and receptors. J. Neurochem. 117, 333–345.

Vendel, E., Rottschäfer, V., de Lange, E.C.M., 2019. The need for mathematical modelling of spatial drug distribution within the brain. Fluids. Barriers. CNS. 16, 12.

Wang, Y., Welty, D.F., 1996. The simultaneous estimation of the influx and efflux blood-brain barrier permeabilities of gabapentin using a microdialysis-pharmacokinetic approach. Pharm. Res. 13, 398–403.

Yamamoto, Y., Danhof, M., de Lange, E.C.M., 2017a. Microdialysis: the key to physiologically based model prediction of Human CNS target site concentrations. AAPS. J. 19, 891–909.

Yamamoto, Y., Välitalo, P.A., Huntjens, D.R., Proost, J.H., Vermeulen, A., Krauwinkel, W., Beukers, M.W., van den Berg, D.J., Hartman, R., Wong, Y.C., Danhof, M., van Hasselt, J.G.C., de Lange, E.C.M., 2017b. Predicting drug concentration-time profiles in multiple CNS compartments using a comprehensive physiologically-based pharmacokinetic model. CPT Pharmacomet. Syst. Pharmacol. 6, 765–777.

Yang, M., Xu, X., 2022. Important roles of transporters in the pharmacokinetics of antiviral nucleoside/nucleotide analogs. Expert. Opin. Drug Metab. Toxicol. 18, 483–505.

Zhang, D., Hop, C., Patilea-Vrana, G., Gampa, G., Seneviratne, H.K., Unadkat, J.D., Kenny, J.R., Nagapudi, K., Di, L., Zhou, L., Zak, M., Wright, M.R., Bumpus, N.N., Zang, R., Liu, X., Lai, Y., Khojasteh, S.C., 2019. Drug concentration asymmetry in tissues and plasma for small molecule-related therapeutic modalities. Drug Metab. Dispos. 47, 1122–1135.

Zhang, M., Vuist, I.M., Rottschäfer, V., de Lange, E.C., 2024. Exploring Kp,uu,BBB values smaller than unity in remoxipride: a physiologically-based CNS model approach highlighting brain metabolism in drugs with passive blood-brain barrier transport. Eur. J. Pharm. Sci: Off. J. Eur. Fed. Pharm. Sci. 203, 106883.

Zhang, Y., Appelkvist, E.L., Kristensson, K., Dallner, G., 1996. The lipid compositions of different regions of rat brain during development and aging. Neurobiol. Aging 17, 869–875.